Published in final edited form as:
J Pharm Biomed Anal. 2013 January 25; 73: 29–34. doi:10.1016/j.jpba.2012.03.033.

Thermal stability of the prototypical Mn porphyrin-based superoxide dismutase mimic and potent oxidative-stress redox modulator Mn(III) *meso*-tetrakis(*N*-ethylpyridinium-2-yl)porphyrin chloride, MnTE-2-PyP^{5+}

Victor H. A. Pinto[1], **Dayse CarvalhoDa-Silva**[2], **Jonas L. M. S. Santos**[1], **Tin Weitner**[3], **Maria Gardênnia Fonseca**[1], **Maria Irene Yoshida**[2], **Ynara M. Idemori**[2], **Ines Batinić-Haberle**[3], and **Júlio S. Rebouças**[1,*]

[1]Departamento de Química, CCEN, Universidade Federal da Paraíba, João Pessoa, PB 58051-900, Brazil

[2]Departamento de Química, ICEx, Universidade Federal de Minas Gerais, Belo Horizonte, MG 31270-900, Brazil

[3]Department of Radiation Oncology, Duke University Medical Center, Durham, NC 27010, U.S.A

Abstract

Cationic Mn porphyrins are among the most potent catalytic antioxidants and/or cellular redox modulators. Mn(III) *meso*-tetrakis(*N*-ethylpyridinium-2-yl)porphyrin chloride (MnTE-2-PyPCl$_5$) is the Mn porphyrin most studied *in vivo* and has successfully rescued animal models of a variety of oxidative stress-related diseases. The stability of an authentic MnTE-2-PyPCl$_5$ sample was investigated hereon by thermogravimetric, derivative thermogravimetric, and differential thermal analyses (TG/DTG/DTA), under dynamic air, followed by studies at selected temperatures to evaluate the decomposition path and appropriate conditions for storage and handling of these materials. All residues were analyzed by thin-layer chromatography (TLC) and UV-vis spectroscopy. Three thermal processes were observed by TG/DTG. The first event (endothermic) corresponded to dehydration, and did not alter the MnTE-2-PyPCl$_5$ moiety. The second event (endothermic) corresponded to the loss of EtCl (dealkylation), which was characterized by gas chromatography-mass spectrometry. The residue at 279 °C had UV-vis and TLC data consistent with those of the authentic, completely dealkylated analogue, MnT-2-PyPCl. The final, multi-step event corresponded to the loss of the remaining organic matter to yield Mn_3O_4 which was characterized by IR spectroscopy. Isothermal treatment at 188 °C under static air for 3 h yielded a mixture of partially dealkylated MnPs and traces of the free-base, dealkylated ligand, H_2T-2-PyP, which reveals that dealkylation is accompanied by thermal demetallation under static air conditions. Dealkylation was not observed if the sample was heated as a solid or in aqueous solution up to ~100 °C. Whereas moderate heating changes sample composition by loss of H_2O, the dehydrated sample is indistinguishable from the original sample upon dissolution in water, which indicates that catalytic activity (on Mn basis) remains unaltered. Evidently, dealkylation at high temperature compromises sample activity.

*Author for correspondence:, Dr. Júlio S. Rebouças, Departamento de Química, Centro de Ciências Exatas e da Natureza, Universidade Federal da Paraíba, João Pessoa, PB 58051-900, Brazil, Tel./Fax: +55-83-3216-7433, jsreboucas@quimica.ufpb.br.

Keywords

Porphyrin; Thermal Analysis; Antioxidant; SOD mimic; Dealkylation

1. Introduction

Cationic Mn porphyrins (MnPs) are among the most active classes of superoxide dismutase mimics [1-5]. These therapeutics, initially developed as catalytic antioxidant agents, are now regarded as potent modulators of the redox cycle with reactive oxygen and nitrogen species (*e.g.*, superoxide and peroxynitrite) and modulate several redox-dependent transcription factors (*e.g.*, NF-κB, HIF-1α, VEGF, AP-1, and p53) [1-4], affecting, thus, a variety of inflammatory, angiogenic, and oncogenic pathways [3,6]. The prototypical cationic Mn porphyrin most studied in vivo, Mn(III) *meso*-tetrakis(*N*-ethylpyridinium-2-yl)porphyrin chloride (MnTE-2-PyPCl$_5$, Fig. 1) has been efficacious in many animal models of oxidative stress-related diseases and injuries [1-4], such as diabetes [7] and radiation injury [8], and as an adjunct in cancer pain management (reversal of morphine tolerance) [9] as well as cancer therapy [4,6]. Master drug file for MnTE-2-PyPCl$_5$ has been filed with the U.S. Food and Drug Administration (FDA) and the toxicity studies needed for Investigational New Drug filing with FDA are in progress [3].

We have previously disclosed in this *Journal* [10] simple analytical techniques, which included thin-layer chromatography (TLC) and UV–vis spectroscopy, that could be used routinely to check the overall quality of MnPs, in particular, to detect the presence of unwanted partially alkylated (mono-, di-, and tri-alkylated species) contaminations. Quantification of residual manganese species, which represent other class of contaminants plaguing Mn porphyrin studies and with critical biological/pharmacological implications [11-13], has also been addressed [11]. Although the stability of MnTE-2-PyPCl$_5$ toward acid hydrolysis, Mn loss, and oxidative degradation has been regularly addressed in the literature [1-3], the thermal stability of MnTE-2-PyPCl$_5$, which is an aspect needed for further development of this compound into clinics, has been largely overlooked. In fact, no study on the thermal stability of any Mn porphyrin-based experimental therapeutics has been reported so far. We present hereon a thermal study on MnTE-2-PyPCl$_5$ by thermogravimetric techniques and differential thermal analysis. Studies of the intermediates and residues were conducted to characterize the proposed decomposition steps.

2. Materials and methods

2.1. General

N,N-dimethylformamide (Janssen Chimica) was distilled under reduced pressure. Deionized water was used throughout this work. All other chemicals (Frontier Scientific, TCI America, Aldrich, Merck, or Synth) were of reagent grade and used as purchased. MnTE-2-PyPCl$_5$·11H$_2$O was prepared and purified as previously described [14], except that the solid was not subjected to vacuum drying under P_2O_5 [14,15]; instead, it was suction-dried in a fritted disk at ambient conditions [10]. The current procedure led to a material containing 11 waters of hydration, as indicated by thermogravimetric analysis (Section 3.1); this number of water molecules differs from that of the previously reported MnTE-2-PyPCl$_5$·4H$_2$O [14] or MnTE-2-PyPCl$_5$·5H$_2$O [15] samples as no attempt was made here to isolate the MnP sample under more stringent drying conditions. Of note, Mn(III) *N*-alkylpyridylporphyrins are invariably isolated as amorphous hydrated solids and the number of waters of hydration is difficult to reproduce from batch-to-batch [1]; suction-dried or lyophilized samples containing 10-20 molecules of water have been routinely isolated [1,16-18] (Batinić-Haberle Laboratories, unpublished data). Characterization of MnTE-2-PyPCl$_5$·11H$_2$O by UV-vis

spectroscopy, ESI-MS, and thin layer chromatography (TLC) yielded data identical to those previously described [10]. MnT-2-PyPCl was prepared as reported and showed spectral features consistent with published data [19].

TLC was carried out in aluminum-backed silica-gel sheets with 254 nm fluorescent indicator (Whatman 4420 222) eluted with a sat. $KNO_{3(aq)}$–H_2O–MeCN (1:1:8, v/v/v) mixture as reported elsewhere [10]. UV-vis spectra (190-900 nm) were recorded in HP-8453 diode-array or Shimadzu UV-1800 spectrophotometers. ESI-MS data were obtained in an Applied Biosystems MDS Sciex 3200 Q Trap LC/MS/MS as reported elsewhere [10]. Fourier-Transform Infrared Spectroscopy (FTIR) was carried out in KBr pellets using Shimadzu IR-Prestige-21 or Thermo Scientific Nicolet 6700 FTIR spectrophotometers. Gas chromatography-mass spectrometry (GC-MS) data were obtained in a Shimadzu GC coupled with a Shimadzu QP2010S mass spectrometer using a Restek Rtx-5 column (30 m × 0.25 mm × 0.25 μm), column He flow of 1.2 ml/min, injector port at 100 °C, and initial oven temperature of 40 °C (for 10 min) with heating rate of 5 °C/min up to a final temperature of 100 °C (for 2 min).

2.2. Thermal analyses

Thermogravimetric (TG), Derivative Thermogravimetric (DTG) and Differential Thermal Analyses (DTA) were carried out in two different Simultaneous DSC-TGA thermal analyzers by TA Instruments SDT 2960 and Shimadzu DTG-60. The analyses were performed from 25 to 900/950 °C, in alumina crucibles, under dynamic air atmosphere with flow rate of 110 cm^3/min and heating rate of 10 °C/min. Independent runs stopped at 110 °C, 279 °C, and 565 °C were carried out for isolation of intermediate residues. Intermediate and final residues were analyzed by TLC, and FTIR and UV-vis spectroscopies; the resulting data were compared with those of appropriate standards.

2.3. Isothermal bulk heating experiments on sand/oil baths

Approx. 3 mg of the MnP sample was placed inside a test tube, which was then immersed in an oil or sand bath at 70, 100, or 188 °C for 3 h under static 1 atm air atmosphere. All residues were analyzed by TLC and UV-vis spectroscopy. Additionally, ~0.5 mg of the MnP sample in a 1.8 ml Wheaton-type vial tightly closed with screw-cap and a Teflon-faced silicon septum was heated at 188 °C for 3 hours, after which 0.1 ml of the gas headspace was withdrawn with a gas-tight Hamilton syringe and analyzed by GC-MS.

2.4. Thermal studies on a melting point apparatus

Visual inspection of the modifications that the sample went through during the thermal events was carried out using a melting point apparatus Gehaka model PF 1500 Farma with sample packed in a capillary tube. Once the instrument was stabilized at 50 °C, the tube was heated at 5 °C/min up to 250 °C or 350 °C. All residues were analyzed by TLC and UV-vis spectroscopy.

3. Results and discussion

Heating MnTE-2-$PyPCl_5$·$11H_2O$ under static air in a melting point apparatus allowed visualization of two processes: dehydration and decomposition, which were later confirmed by thermogravimetric analyses. The dehydration was observed by water condensation on the colder top walls of the capillary tube when the closed end of the tube reached temperature in the 100-110 °C range. Heating the sample up to 192-202 °C provided indirect evidence of gas release by physical projection of solid particles toward the open end of the capillary tube.

The thermal stability studies of MnTE-2-PyPCl$_5$·11H$_2$O were carried out independently in two different laboratories (UFPB and UFMG) and produced identical results. The TG/DTG/DTA analyses are presented in Figure 2 while the related data are compiled in Table 1, along with mass loss assignment. The thermogravimetric events under dynamic air were associated with 3 major processes: dehydration, dealkylation, and organic matter degradation to yield Mn oxide as final residue at 900 or 950 °C. The thermal decomposition of the sample was also studied under static air, using less controlled settings, by heating MnTE-2-PyPCl$_5$·11H$_2$O isothermically in a test tube immersed in a sand or oil bath. Different heating conditions (controlled TG settings versus bath test tube heating) revealed differences in the nature of the thermal decomposition intermediates (Section 3.2).

3.1. Process I: dehydration

The first thermal process to which MnTE-2-PyPCl$_5$·11H$_2$O undergoes is an endothermic event in the 26–134 °C range with DTG peak at 67.5 °C (Fig. 2, region I; Table 1), which corresponds to a weight loss of 17.15% and is consistent with the calculated loss of 11 water molecules. Dehydration of the tetracationic free-ligand porphyrin, H$_2$TM-4-PyPCl$_4$·8H$_2$O, under nitrogen atmosphere takes place in a closely related temperature range [20]. TLC and UV-vis analyses of the TG intermediate residue collected at 110 °C (Fig. 2, point “a”) under dynamic atmosphere or the solids resulting from test tube isothermic heating at 70 °C or 100 °C under static atmosphere revealed that the MnTE-2-PyPCl$_5$ chromophore remained intact. Dissolution of these materials in water resulted in solutions that produced a single spot on TLC plates, co-eluted with the original MnP sample, and had UV-vis spectral features indistinguishable from those of MnTE-2-PyP$^{5+}_{(aq)}$ (Fig. S1 in the Supplementary Materials) [10]. This indicates that whereas water removal changed the overall formulation of the solid sample, the solution SOD catalytic activity (on Mn basis) is, thus, preserved.

3.2. Process II: dealkylation

Following dehydration, the next thermal event is characterized by an endothermic mass drop in the 134–279 °C temperature range (Fig. 2, region II; Table 1), which amounts to 22.50 % weight loss and has been assigned to the complete dealkylation of MnTE-2-PyPCl$_5$ *via* loss of ethyl chloride to yield MnT-2-PyPCl (Fig. 1). Characterization of EtCl was accomplished by GC-MS by analyzing the headspace of a closed vial containing MnTE-2-PyPCl$_5$·11H$_2$O and heated at 188 °C. The chromatogram was marked by a single peak whose mass spectrum (Fig. S2 in the Supplementary Material) showed two clusters corresponding to the EtCl molecular ion (m/z 64, [M]$^+$) and its fragment (m/z 49,[M–CH$_3$]$^+$), both with isotopic distribution consistent with the presence of one Cl-atom. The MS spectrum matched quantitatively that of EtCl in the NIST library, with 98% of similarity. The UV-vis and TLC-SiO$_2$ data of the solid collected at 279 °C (Fig. 2, point “b”) are consistent with those of the dealkylated analogue MnT-2-PyPCl [19] (Fig. 3). The formation of gaseous EtCl represents the reverse of an alkylation reaction and is consistent with the gas release observed in the melting point apparatus. Additionally, the loss of MeCl was previously described in the related porphyrin ligand H$_2$TM-4-PyPCl$_4$ [20]. The removal of alkyl halides from for other non-porphyrin *N*-alkylpyridinium and *N*-alkylimidazolium salts [21-23] has been described as endothermic events that take place in a temperature range closely related to that found for MnTE-2-PyPCl$_5$·11H$_2$O (Table 1). It is worth noting that the TLC-SiO$_2$ analysis of the 279 °C intermediate (Fig. 2, point “b”) showed MnT-2-PyPCl as the major spot, but traces of both the mono and the di-alkylated species, which resulted from partial dealkylation of MnTE-2-PyPCl$_5$ and whose retention factor (R$_f$) data were comparable to those in the literature [10], were observed. This is consistent with the DTG curve profile (Fig. 2, region II) that indicates that EtCl loss does not take place as a single event, but as at least three very closely related ones; the loss of even one single ethyl group (as EtCl) would result in a compound of limited redox modulation potency [1,2]. Whereas partially alkylated

ortho Mn(III) *N*-alkylpyridylporphyrins have increased lipophilicity [10,16,17], which may be beneficial for tissue biodistribution/accumulation and cellular uptake [24,25], the reduced Mn(III)/Mn(II) reduction potential [16] and poorer electrostatic guidance for superoxide and peroxynitrite anion approach [26-28] associated with a lower overall cationic charge, translates into lower SOD activity [14,26-28] and peroxynitrite scavenging potency [13]. Contrary to the previous temperature-induced, reversible dehydration event, which has little impact in a biological setting as the sample is administered *in vivo* as aqueous formulations [1-4,8,9,25], the dealkylation process is irreversible and means irreparable loss of biological activity; MnT-2-PyPCl is not an SOD mimic [29]. As expected, no dealkylation was observed if the sample was heated up to 100 °C for 3 h either as solid or aqueous solution; in addition to the temperature being relatively low for the dealkylation process, it is likely that solvation stabilizes the *N*-ethylpyridinium moiety by keeping the chloride anions apart from the ethyl groups, which prevents, thus, EtCl elimination.

Heating MnTE-2-PyPCl$_5$·11H$_2$O isothermically at 188 °C under static atmosphere, produced a residue that was partially soluble in water, partially soluble in CHCl$_3$ and contained a small amount of a material that was insoluble in H$_2$O, CHCl$_3$, MeOH, and MeCN. The TLC and UV-vis analyses revealed that the 188 °C residue contained a mixture for partially dealkylated species (mono and diethylated MnT-2-PyPCl species [10]) along with traces of the demetallated porphyrin H$_2$T-2-PyP. The presence of H$_2$T-2-PyP in the CHCl$_3$ extract was characterized by TLC co-elution with an authentic sample, by UV-vis spectroscopy (Soret band at 412 nm in MeOH, Fig. 3) and by its fluorescent nature when observed under long-wavelength UV lamp. In addition to MnT-2-PyPCl (major species), the mono and dialkylated Mn derivatives were present, but no alkylated free-base ligand (such as H$_2$TE-2-PyPCl$_4$ or less alkylated analogues) were observed, indicating that demetallation took place after dealkylation. Under static atmosphere conditions, the released EtCl is not flushed from the system and would remain in close contact with the sample. The thermal dehydrochlorination of EtCl is likely to happen at longer heating contact time to yield HCl [30-32], which may be involved in the demetallation of the sample. As Mn(III) porphyrins are stable toward acid-demetallation [26], some *in situ* reduction to Mn(II) species cannot be ruled out and may explain the demetallation [26]. Although the observation of H$_2$T-2-PyP is intriguing, investigation on the origin of this species was not pursued further, as H$_2$T-2-PyP amounts to ~5 % (at best) in the 188 °C residue. Interestingly, when a sample of MnTE-2-PyPCl$_5$·11H$_2$O was heated under static atmosphere at 250 °C, TLC and UV-vis data (Fig. 3) showed that, in addition to MnT-2-PyPCl and traces of monoethylated MnP species, enrichment in H$_2$T-2-PyP was observed along with a greater deal of intractable residue.

Whereas in all experiments conducted at high temperature under dynamic atmosphere (TG) conditions no demetallation was observed, under static atmosphere conditions dealkylation was accompanied by some thermally-assisted demetallation, which is likely a result of the formation of reactive species, such as HCl [30], *via* the EtCl product accumulated within the system. This suggests that any attempt to prepare an anhydrous MnTE-2-PyPCl$_5$ sample may be tainted by dealkylation and such procedure, if attempted, should be carried out at a reasonable system purge with air or any suitable inert gas in order to avoid that demetallation takes place concomitantly with the too-undesirable dealkylation.

3.3. Process III: porphyrin decomposition

The third process in the thermal degradation of MnTE-2-PyPCl$_5$·11H$_2$O takes place as a complex multi-step event from 279 to 901 °C (Fig. 2, region III; Table 1) that results in the loss of the organic matter and the remaining chloride to yield manganese oxide as residue (see Section 3.4). Closer inspection of the DTG curve in this temperature range suggests that this region III could be further divided in four smaller sub-regions (IIIa to IIId) as indicated in Fig. 2 and Table 1. The greater weight loss in the sample occurs in the sub-region IIIc,

from 479 to 606 °C, with DTG peak at 521.4 °C. The large exothermic peak in DTA curve at 521.4 °C associated with this event is consistent with a combustion process. The TG intermediate residue collected at 565 °C (Fig. 2, point "c"), at the end of sub-region IIIc, is insoluble in most common solvents but dissolves in $HNO_{3(conc)}$ to yield an off-white solution, whose UV-vis spectra reveal the absence of porphyrin or any tetrapyrrolic conjugated compound. In fact, heating MnTE-2-PyPCl$_5$·11H$_2$O up to 350 °C (sub-region IIIa) in the melting point apparatus, led to a material that showed no porphyrin spectra, indicating that the porphyrin core integrity was already compromised at the beginning of region III. The weight loss associated with sub-region IIId (2.91 %, Table 1) is curiously close to that calculated (3.04 %) for the loss of the single chloride counter-ion remaining in the MnP sample (after removal of the other four chlorides as EtCl), but we were unable to find a related system in the literature to substantiate such a speculation.

3.4. Final residue

The final residues of the thermogravimetric studies on MnTE-2-PyPCl$_5$·11H$_2$O were collected at 900 °C or 950 °C. Either residues gave essentially the same IR spectra in the 400–800 cm^{-1} region, where characteristic Mn-O stretches of manganese oxide species usually appear [33,34]. Comparison of the IR data of the final residues with those of standard manganese oxides, namely, MnO_2, Mn_2O_3, Mn_3O_4, and MnO (Fig. S3 in Supplementary Material), suggested that the final TG residue could be tentatively assigned to Mn_3O_4, which is also in agreement with the theoretical weight % of the TG curve (Table 1). Whereas the formation of Mn_3O_4 may occur in the temperature range used to collect the residue, the contribution of Mn_2O_3 or even a formulation considering the residue as a mixture of Mn oxides cannot be completely ruled out at this point as vibrational data on Mn oxides are markedly dependent on polymorphism composition and the grain size of the material [33-35], which are properties that were not investigated in this work. The formulation of the residue as Mn_3O_4, Mn_2O_3, or a mixture of both is consistent with the well established temperature-dependent stability of the various Mn oxides [36-38].

4. Conclusions

The thermal decomposition of MnTE-2-PyPCl$_5$·11H$_2$O takes place in three major successive thermal processes under dynamic air at 1 atm: the first event, in the 26–134 °C range (DTG peak at 67.5 °C), is endothermic and corresponds to the loss of the waters of hydration; the second event, in the 134–279 °C range (DTG peak at 201.7 °C), is also endothermic and corresponds to the loss of the ethyl chloride moieties (as EtCl), *i.e.*, porphyrin dealkylation; the last event, in the 279–901 °C range (DTG peaks at 391.8, 453.8, 521.4, 698.5 °C), is a multiple, stepwise process that corresponds to the loss of the remaining organic matter and oxygen incorporation into the decomposition residue to yield manganese oxides. Heating MnTE-2-PyPCl$_5$·11H$_2$O up to ~100 °C change its composition (by loss of water molecules), but with no effect onto the intrinsic catalytic SOD activity (per Mn). Heating the sample under static atmosphere (at constant, high temperature) may lead to both dealkylation and demetallation.

Supplementary Material

Refer to Web version on PubMed Central for supplementary material.

Acknowledgments

This work was funded by Governmental Agencies from Brazil (CNPq: 474663/2010-8, 305713/2010-8, 306652/2009-9, 477971/2008-3; FAPEMIG: PPM-00475-09) and the U.S. (NIH: U19AI067798). Infrastructure support from FINEP (Pro-Infra), UFMG, and PRPG-UFPB is greatly appreciated. Student scholarships from CAPES (V.H.A.P.) and CNPq (D.C.S. and J.L.M.S.S.) are acknowledged. We thank Laboratório de Combustíveis e

Materiais (UFPB) for allowing access to the TG/DTG/DTA instruments. Access to the Thermo Scientific FTIR spectrophotometer was granted by Dr. Mark D. Walters at the Duke University Shared Materials Instrumentation Facility and is acknowledged. We thank Dr. Artak Tovmasyan and Dr. Ivan Spasojević (Duke University Cancer Institute Shared Pharmacology Lab) for the ESI-MS data and Dr. Juliana A. Vale (UFPB) for GC-MS analyses.

References

1. Batinić-Haberle, I.; Rebouças, JS.; Benov, L.; Spasojević, I. Chemistry, Biology and Medical Effects of Water-Soluble Metalloporphyrins. In: Kadish, KM.; Smith, KM.; Guilard, R., editors. Handbook of Porphyrin Science. Vol. 11. World Scientific Publishing; New York: 2011. p. 291-394.
2. Batinić-Haberle I, Rebouças JS, Spasojević I. Superoxide Dismutase Mimics: Chemistry, Pharmacology and Therapeutic Potential. Antioxid Redox Signal. 2010; 13:877–918. [PubMed: 20095865]
3. Batinić-Haberle I, Rajic Z, Tovmasyan A, Rebouças JS, Ye X, Leong KW, Dewhirst MW, Vujasković Z, Benov L, Spasojević I. Diverse functions of cationic Mn(III) *N*-substituted pyridylporphyrins, recognized as SOD mimics. Free Radic Biol Med. 2011; 51:1035–1053. [PubMed: 21616142]
4. Miriyala S, Spasojević I, Tovmasyan A, Salvemini D, Vujasković Z, StClair D, Batinić-Haberle I. Manganese superoxide dismutase, MnSOD and its mimics. Biochem Biophys Acta. 2012; 1822:794–814. [PubMed: 22198225]
5. DeFreitas-Silva G, Rebouças JS, Spasojević I, Benov L, Idemori YM, Batinić-Haberle I. SOD-like activity of Mn(II) β-octabromo-*meso*-tetrakis(*N*-methylpyridinium-3-yl)porphyrin equals that of the enzyme itself. Arch Biochem Biophys. 2008; 477:105–112. [PubMed: 18477465]
6. Batinić-Haberle I, Spasojević I, Tse HM, Tovmasyan A, Rajic Z, StClair DK, Vujasković Z, Dewhirst MW, Piganelli JD. Design of Mn porphyrins for treating oxidative stress injuries and their redox-based regulation of cellular transcriptional activities. Amino Acids. 2012; 42:95–113. [PubMed: 20473774]
7. Sklavos MM, Bertera S, Tse HM, Bottino R, He J, Beilke JN, Coulombe MG, Gill RG, Crapo JD, Trucco M, Piganelli JD. Redox modulation protects islets from transplant-related injury. Diabetes. 2010; 59:1731–1738. [PubMed: 20413509]
8. Gauter-Fleckenstein B, Fleckenstein K, Owzar K, Jiang C, Rebouças JS, Batinić-Haberle I, Vujasković Z. Early and late administration of MnTE-2-PyP^{5+} in mitigation and treatment of radiation-induced lung damage. Free Radic Biol Med. 2010; 48:1034–1043. [PubMed: 20096348]
9. Batinić-Haberle I, Ndengele MM, Cuzzocrea S, Rebouças JS, Spasojević I, Salvemini D. Lipophilicity is a critical parameter that dominates the efficacy of metalloporphyrins in blocking the development of morphine antinociceptive tolerance through peroxynitrite-mediated pathways. Free Radic Biol Med. 2009; 46:212–219. [PubMed: 18983908]
10. Rebouças JS, Spasojević I, Batinić-Haberle I. Quality of potent Mn porphyrin-based SOD mimics and peroxynitrite scavengers for pre-clinical mechanistic/therapeutic purposes. J Pharm Biomed Anal. 2008; 48:1046–1049. [PubMed: 18804338]
11. Rebouças JS, Kos I, Vujasković Z, Batinić-Haberle I. Determination of residual manganese in Mn porphyrin-based superoxide dismutase (SOD) and peroxynitrite reductase mimics. J Pharm Biomed Anal. 2009; 50:1088–1091. [PubMed: 19660888]
12. Rebouças JS, Spasojević I, Batinić-Haberle I. Pure manganese(III) 5,10,15,20-tetrakis(4-benzoic acid)porphyrin (MnTBAP) is not a superoxide dismutase mimic in aqueous systems: A case of structure-activity relationship as a watchdog mechanism in experimental therapeutics and biology. J Biol Inorg Chem. 2008; 13:289–302. [PubMed: 18046586]
13. Batinic-Haberle I, Cuzzocrea S, Rebouças JS, Ferrer-Sueta G, Mazzon E, Dipaola R, Radi R, Spasojević I, Benov L, Salvemini D. Pure MnTBAP selectively scavenges peroxynitrite over superoxide: Comparison of pure and commercial MnTBAP samples to MnTE-2-PyP in two models of oxidative stress injury, an SOD-specific Escherichia coli model and carrageenan-induced pleurisy. Free Radic Biol Med. 2009; 46:192–201. [PubMed: 19007878]
14. Batinić-Haberle I, Spasojević I, Hambright P, Benov L, Crumbliss AL, Fridovich I. The Relationship Between Redox Potentials, Proton Dissociation Constants of Pyrrolic Nitrogen and *in*

vivo and *in vitro* Superoxide Dismutase Activities of Manganese(III) and Iron(III) Cationic and Anionic Porphyrins. Inorg Chem. 1999; 38:4011–4022.

15. Kachadourian R, Batinić-Haberle I, Fridovich I. Syntheses and Superoxide Dismuting Activities of Partially (1-4) β-Chlorinated Derivatives of Manganese(III) meso-Tetrakis(N-ethylpyridinium-2-yl)porphyrin. Inorg Chem. 1999; 38:391–396.
16. Kos I, Rebouças JS, DeFreitas-Silva G, Salvemini D, Vujaskovic Z, Dewhirst MW, Spasojević I, Batinić-Haberle I. Lipophilicity of potent porphyrin-based antioxidants: Comparison of *ortho* and *meta* isomers of Mn(III) *N*-alkylpyridylporphyrins. Free Radic Biol Med. 2009; 47:72–78. [PubMed: 19361553]
17. Kos I, Benov L, Spasojević I, Rebouças JS, Batinić-Haberle I. High lipophilicity of meta Mn(III) *N*-alkylpyridylporphyrin-based superoxide dismutase (SOD) mimics compensates for their lower antioxidant potency and makes them equally effective as ortho analogues in protecting SOD-deficient *E. coli*. J Med Chem. 2009; 52:7868–7872. [PubMed: 19954250]
18. Batinić-Haberle I, Spasojević I, Stevens RD, Hambright P, Fridovich I. Manganese(III) meso-tetrakis(ortho-N-alkylpyridyl)porphyrins. Synthesis, characterization, and catalysis of $O_2^{\bullet-}$ dismutation. J Chem Soc Dalton Trans. 2002:2689–2696.
19. Rebouças JS, de Carvalho MEMD, Idemori YM. Perhalogenated 2-pyridylporphyrin complexes: synthesis, self-coordinating aggregation properties, and catalytic studies. J Porphyrins Phthalocyanines. 2002; 6:50–57.
20. Carrado, KA.; Anderson, KB.; Grutkoski, PS. Thermal analysis of porphyrin-clay complexes. In: Bein, T., editor. ACS Symposium Series. Vol. 499. American Chemical Society; Washington: 1992. p. 155-165.
21. Zhao T, Sun G. Synthesis and Characterization of Antimicrobial Cationic Surfactants: Aminopyridinium Salts. J Surfactants Deterg. 2006; 9:325–330.
22. Kroon MC, Buijs W, Peters CJ, Whitlam GJ. Quantum chemical aided prediction of the thermal decomposition mechanisms and temperatures of ionic liquids. Thermochim Acta. 2007; 465:40–47.
23. Ngo HL, LeCompte K, Hargens L, McEwen AB. Thermal properties of imidazolium ionic liquids. Thermochim Acta. 2000; 357–358:97–102.
24. Pollard JM, Rebouças JS, Durazo A, Kos I, Fike F, Panni M, Gralla EB, Valentine JS, Batinić-Haberle I, Gatti RA. Radioprotective effects of manganese-containing superoxide dismutase mimics on ataxia telangiectasia cells. Free Radic Biol Med. 2009; 47:250–260. [PubMed: 19389472]
25. Spasojević I, Kos I, Benov LT, Rajic Z, Fels D, Dedeugd C, Ye X, Vujaskovic Z, Rebouças JS, Leong KW, Dewhirst MW, Batinić-Haberle I. Bioavailability of metalloporphyrin-based SOD mimics is greatly influenced by a single charge residing on a Mn site. Free Radic Res. 2011; 45:188–200. [PubMed: 20942564]
26. Rebouças JS, DeFreitas-Silva G, Spasojević I, Idemori YM, Benov L, Batinić-Haberle I. The impact of electrostatics in redox modulation of oxidative stress by Mn porphyrins: Protection of SOD-deficient *Escherichia coli* via alternative mechanism where Mn porphyrin acts as a Mn-carrier. Free Radic Biol Med. 2008; 45:201–210. [PubMed: 18457677]
27. Spasojević I, Batinić-Haberle I, Rebouças JS, Idemori YM, Fridovich I. Electrostatic contribution in the catalysis of O_2^- dismutation by superoxide dismutase mimics. Mn(III)TE-2-PyP^{5+} *vs* Mn(III)Br_8T-2-PyP^+ J Biol Chem. 2003; 278:6831–6837. [PubMed: 12475974]
28. Rebouças JS, Spasojević I, Tjahjono DH, Richaud A, Méndez F, Benov L, Batinić-Haberle I. Redox modulation of oxidative stress by Mn porphyrin-based therapeutics: The effect of charge distribution. Dalton Trans. 2008:1233–1242. [PubMed: 18283384]
29. Spasojević I, Batinić-Haberle I. Manganese(III) complexes with porphyrins and related compounds as catalytic scavengers of superoxide. Inorg Chim Acta. 2001; 317:230–242.
30. Gutmann H, Kertes AS. Thermal stability of long-chain aliphatic amine salts. J Inorg Nucl Chem. 1969; 31:205–211.
31. Barton DHR, Howle KE. The kinetics of the dehydrochlorination of substituted hydrocarbons. Part III. The mechanisms of the thermal decompositions of ethyl chloride and of 1:1-dichloroethane. J Chem Soc. 1949:165–169.

32. Smith, MB.; March, J. March's Advanced Organic Chemistry: Reactions, Mechanisms, and Structure. 6th. John Wiley & Sons; Hoboken: 2007. p. 1530-1532.

33. Al Sagheer FA, Hasan MA, Pasupulety L, Zaki MI. Low-temperature synthesis of Hausmannite Mn_3O_4. J Mat Sci Lett. 1999; 18:209–211.

34. Salavati-Niasari M, Mohandes F, Davar F, Saberyan K. Fabrication of chain-like Mn_2O_3 nanostructures via thermal decomposition of manganese phthalate coordination polymers. Appl Surface Sci. 2009; 256:1476–1480.

35. Chen ZW, Lai JKL, Shek CH. Influence of grain size on the vibrational properties in Mn_2O_3 nanocrystals. J Non-Cryst Solids. 2006; 352:3285–3289.

36. Li L, He M, Zhang A, Zhou J. A study on non-isothermal kinetics of the thermal decompositions of β-manganese dioxide. Thermochim Acta. 2011; 523:207–213.

37. Tinsley DM, Sharp JH. Thermal analysis of manganese dioxide in controlled atmospheres. J Thermal Anal. 1971; 3:43–48.

38. Bish DL, Post JE. Thermal behavior of complex, tunnel-structure manganese oxides. Am Mineral. 1989; 74:177–186.

Abbreviations

H_2T-2-PyP	*meso*-tetrakis(2-pyridyl)porphyrin
H_2TE-2-PyPCl_4	*meso*-tetrakis(*N*-ethylpyridinium-2-yl)porphyrin
MnTE-2-PyPCl_5	Mn(III) *meso*-tetrakis(*N*-ethylpyridinium-2-yl)porphyrin chloride (also known as AEOL10113 and FBC-007)
MnP	Mn(III) porphyrin
MnT-2-PyPCl	Mn(III) *meso*-tetrakis(2-pyridyl)porphyrin chloride
SOD	superoxide dismutase

Highlights

- MnTE-2-PyPCl$_5$ is the Mn porphyrin-based therapeutics most studied *in vivo*
- Heating sample under static atmosphere may lead to dealkylation and demetallation
- Thermal events observed: dehydration, dealkylation, demetallation, and combustion
- Dealkylation does not occur up to 100 °C, preserving thus MnTE-2-PyP^{5+} activity

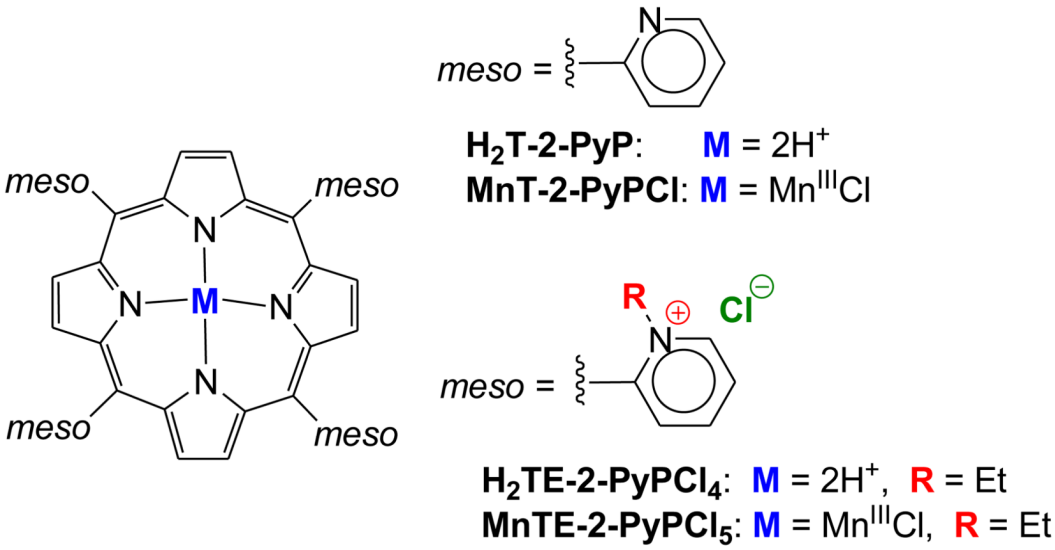

Figure 1.
Structure of 2-*N*-pyridyl-based porphyrins and Mn porphyrins.

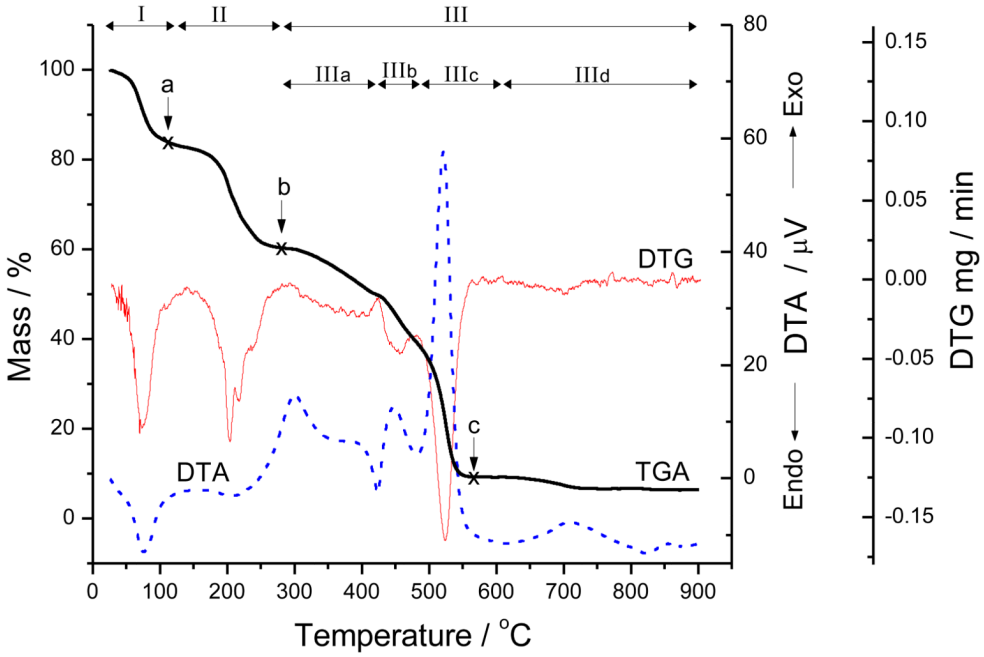

Figure 2.
TG, DTG, and DTA curves for MnTE-2-PyPCl$_5$·11H$_2$O under dynamic air at a heating rate of 10 °C/min.

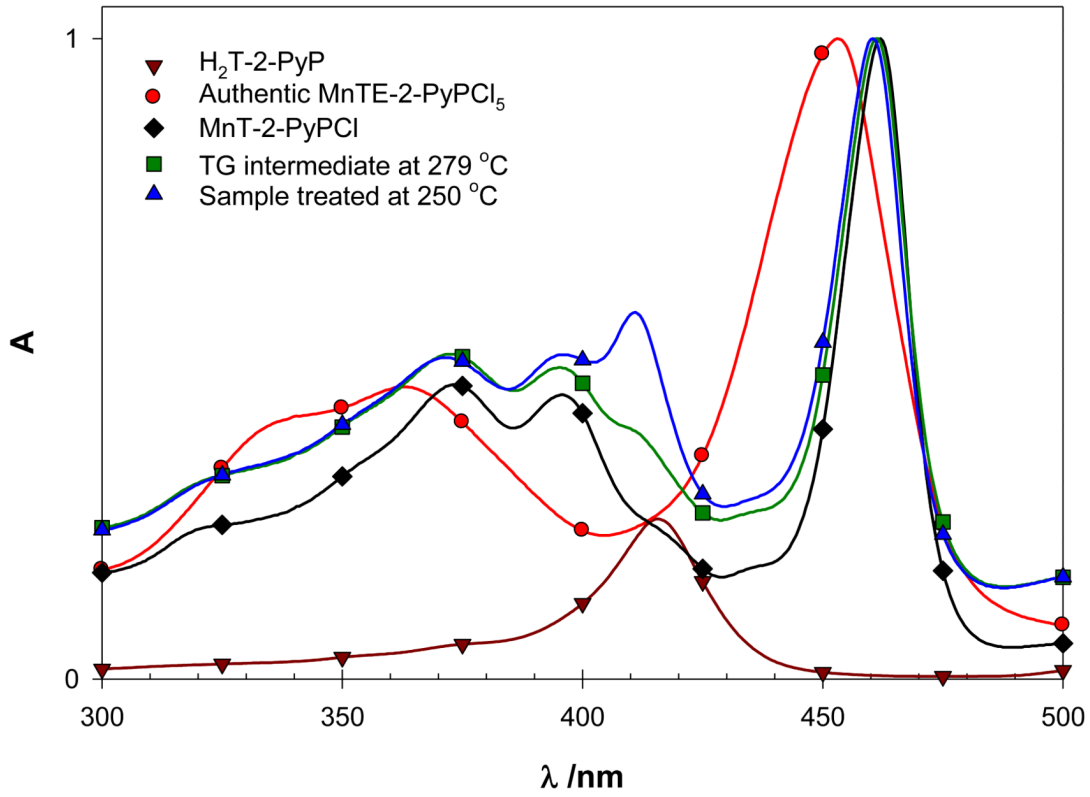

Figure 3.
UV-vis spectra (MeOH) of H_2T-2-PyP, MnTE-2-PyPCl_5, MnT-2-PyPCl, the TG intermediate decomposition product at 279 °C, and the sample heated in the capillary tube (under static atmosphere) up to 250 °C.

Table 1

Thermal analysis data for MnTE-2-PyPCl$_5$· 11H$_2$O under dynamic 1 atm air atmosphere (110 cm^3/min) at a heating rate of 10 °C/min.

Process	TG/DTG						DTA[a]	Assignment
	Temperature, °C				% Weight loss		DTA peak, °C	
	Range	T_{onset}	T_{offset}	DTG peak	Exp	Calcd		
I	26 – 134	56.4	90.1	67.5	17.15	17.04	75.6 (endo)	Loss of waters of hydration (–11 H_2O)
II	134 –279	186.4	228.6	201.7	22.50	22.15	205.2 (endo)	Loss of EtCl (–4 EtCl)
III IIIa	279 – 421	330.5	411.4	391.8	10.42		300.1 (exo)	Loss of remaining organic matter and
IIIb	421 – 479	432.9	463.1	453.8	10.18		423.6 (endo), 447.4 (exo)	incorporation of oxygen to yield
IIIc	479 – 606	506.2	538.8	521.4	30.43		481.9 (endo), 521.4 (exo)	residual Mn oxide
IIId	606 – 901	688.7	722.7	698.5	2.91		709.9 (exo)	(Loss of remaining chloride?)
	270 – 901				53.94	54.25		
Residue	902	–	–	–	6.35	6.56	-	Mn_3O_4 as final residue

[a]Endo stands for an endothermic event, whereas exo stands for an exothermic event.